Archives of Materials Science and Engineering

Volume 117
Issue 1
September 2022
Pages 34-41

International Scientific Journal
published monthly by the
World Academy of Materials
and Manufacturing Engineering

DOI: 10.5604/01.3001.0016.1395

Effect of fibre laser welding parameters on the microstructure and weld geometry of commercially pure titanium

M.M. Abdulridha, A.S.J.A.Z. Jilabi *
Materials Engineering Faculty, University of Babylon, Hilla, Iraq
* Corresponding e-mail address: sameeakilabi@gmail.com
ORCID identifier: https://orcid.org/0000-0003-3636-3738 (M.M.A.)

ABSTRACT

Purpose: The primary purpose of the study was the metallurgical characterization of laser welds. The weldability of commercial production of pure titanium and titanium alloy (CP-Ti) has also been examined.

Design/methodology/approach: In this research, the laser fibre method was used to weld sheets of pure titanium, and then microscopy and scanning electron microscopy were used to study the changes in the microstructure, the depth of weld penetration and the width of the weld area with changing welding parameters.

Findings: The results proved that increasing the laser power significantly increases the depth of weld penetration and weld width. When the heat input is increased, the shape of the weld pool changes from a V shape to an hourglass shape. It was also observed that the depth of the crater formed increases with the increase in the laser power due to the increase in the melting and evaporation of the weld metal. Increasing the welding speed also has a negative impact on the weld geometry because it reduces the heat input and absorption of laser energy by the weld metal and thus reduces the melting of the metal. The microstructure of the fusion zone consists of acicular α. Fine grains formed in the weld centre at low heat input; the granules became columnar-like. Since commercially pure titanium contains a small amount of beta-phase stabilizers, the cooling rate is extremely high for martensite to occur.

Research limitations/implications: In the future, it is recommended to study the effect of changing welding parameters on the mechanical properties of pure titanium because of its great importance in industrial and medical applications.

Originality/value: Studying the effect of changing laser power and welding speed on the metallurgical properties of pure titanium, and consequently its effect on the mechanical properties of welds.

Keywords: Fibre laser welding, Laser power, Welding speed, CP titanium, Depth penetration weld, Weld width

Reference to this paper should be given in the following way:

M.M. Abdulridha, A.S.J.A.Z. Jilabi, Effect of fibre laser welding parameters on the microstructure and weld geometry of commercially pure titanium, Archives of Materials Science and Engineering 117/1 (2022) 34-41. DOI: https://doi.org/10.5604/01.3001.0016.1395

MATERIALS MANUFACTURING AND PROCESSING

1. Introduction

Since of its remarkable mix of characteristics, titanium, as well as its alloys, are one of the greatest engineering materials for industrial applications. They are appealing to numerous industries ranging from structural components to aviation and aerospace applications because of their good formability, corrosion resistance, excellent toughness, fatigue life, and great strength/weight proportion [1]. Titanium alloys have become classified into five categories based on the alloying elements that are present: near-beta alloys, alpha-beta (β) alloys and alpha (α) alloys. These five varieties of titanium alloys have a broad variety of mechanical qualities, allowing enterprises to choose the one that best matches their needs [2]. Although traditional welding processes may be utilized to combine Ti alloy sheets, the material's reduced thermal conductivity and thermal stresses caused by substantial heat inputs throughout welding generally result in workpiece deformation [3]. Deep penetration, limited bead width, and a restricted heating impacted area seem to be common features of the great power density laser beams welding (LBW) technique. The procedures of plasma stream welding and electron beam welding seem to be likewise comparable [4,5]. Gas shielding is critical in laser welding titanium alloys because titanium becomes extremely reactive with nitrogen, oxygen, and hydrogen at high temps, resulting in lattice deformation or weld fractures. [6]. Since titanium undergoes an allotropic phase shift around 882 degrees centigrade, where alpha (HCP) converts into beta, the titanium alloys and titanium microstructure may be quite complicated (BCC). Welding conditions have a great effect on the shape of the weld pool and the microstructure formed in the FZ and the HAZ. When the heat input increases or the welding speed decreases, the shape of the weld pool changes from a V- shape to an hourglass shape [7], The decrease in welding speed leads to a change in the shape of the weld from that of an hourglass to the shape of a nail head, and tendency to trap gases and form porosity at high speeds [8,9]. The heating and rapid cooling during the laser welding process lead to forming three zones FZ, HAZ and BM. The microstructure of commercially pure titanium in the weld zone is composed of a needle-shaped alpha because the cooling rate is insufficient to form martensite because the stabilizing elements of the beta phase are very few. The heat-affected zone can be easily distinguished from the base metal due to the difference in their microstructure. In contrast, the weld zone is difficult to distinguish from the heat-affected zone due to the similarity in the microstructure [8,10].

2. Experimental set-up and materials used

The material used is Grade 2 (CP) with a thickness of 0.3 cm. The specimen's dimensions utilized are 35 mm × 50 mm as shown in Figure 1. The chemical composition of these samples is shown in Table 1. The laser equipment was a YFL-1500, a single mode (1080 nm, continuous waves) fibre laser with an optimum power of 1500 W and a Gaussian beam (Fig. 2). In this experiment, laser power between 600 and 1500 W, and welding speeds of 2-10 mm/s were used. The focusing optical mode has a focal length of 15 cm and a minimum laser spot size of 200 µm. Pure argon (99.9%) has been employed as a shielding gas for all welds with an incidence angle of 45° and a flow rate of 10 l/min to avoid oxidations.

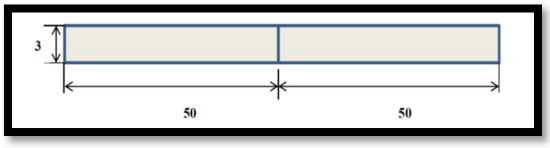

Fig. 1. Dimensions of samples to be joined (in millimetres)

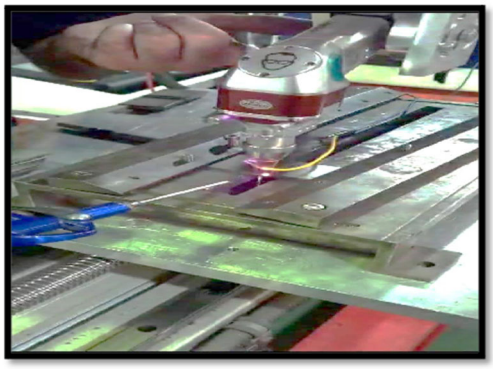

Fig. 2. Fibre laser machine

Table 1.
Chemical analysis of CP-Ti (Grade 2) used in the study

Materials	Chemical analysis, wt.%							
	Ti	Al	Fe	C	O	H	N	V
Grade 2-CP-Ti (nominal)	R	-	Max-0.3	Max-0.08	Max-0.25	Max-0.015	Max-0.03	-
Result	R	-	0.05	0.012	0.092	0.001	0.018	-

Specimens were subsequently prepared for microstructural analysis by mounting them on a thermosetting resin and then grinding them with silicon carbide sheets of various grain sizes (320-1200). After polishing with different particle sizes of diamond paste, the specimens were etched utilizing Kroll's reagent (85ml HO+10 ml HNO_3+5 ml HF), ASTM E407 [11], to achieve a mirror surface. The heat input (HI) in fibre laser welding could be estimated utilizing formula (1) [12]; Table 2 details the parameters employed in the fibre LBW process.

$$HI\left(\frac{J}{mm}\right) = \eta \frac{LaserPower(W)}{WeldingSpeed\left(\frac{mm}{s}\right)} \quad (1)$$

Therefore, it can depend on the experimental technique to calculate the out results, with different input parameters effect, and with low error. Since the experimental was perfect technique can be used to evaluate the out results with various parameters effects with low discrepancies [13-16].

Table 2.
The parameters that were employed with the fibre LBW process

Parameters / No. of samples	Laser power, kW	Welding speed, mm/s	Heat input, J/mm
A1	0.6	10	60
A2	0.9	10	90
A3	1.2	10	120
A4	1.5	10	150
A5	0.6	15	40
A6	0.9	15	60
A7	1.2	15	80
A8	1.5	15	100
A9	0.6	20	30
A10	0.9	20	45
A11	1.2	20	60
A12	1.5	20	75
A13	0.6	25	24
A14	0.9	25	36
A15	1.2	25	48
A16	1.5	25	60

3. Results and discussion

3.1. Microstructural evolution during LBW of Ti alloys

During the LBW processes, the heat source interacts with a specific area of the workpiece material [17]. As a result, the weldment undergoes an extreme temperature gradient that leads to the formation of three separate zones with a heterogeneous microstructure: unaffected base metals (BM), heating-affecting zones (HAZ) and fusion zones (FZ) [18,19], as demonstrated in Figure 3. Despite a clear distinction between the HAZ and BM, the microstructures created in the HAZ and FZ were so identical that the fusion line could not be accurately determined. Instead, the fusion line is approximated based on the location of the weld root and weld toes [20]. The size and shape of the weld pool impact the mechanical properties of the weld joint by controlling the shape and size of the grain [21]. It was noted that the welds have a keyhole penetration style.

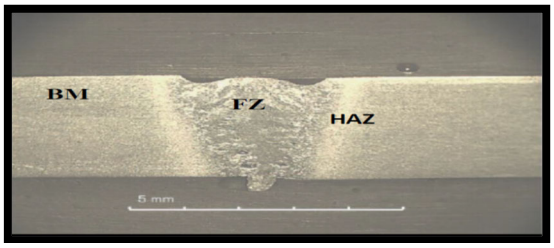

Fig. 3. Weld microstructures of the A8 specimen

In this study, 16 samples of the (CP-Ti) were similarly joined using the fibre laser method in different welding conditions, resulting in different heat inputs. The microstructure and mechanical properties are directly related to the heat input during welding, as it is the main factor for the occurrence of phase transitions. Higher inputs are achieved with higher laser power or lower welding speed and vice versa. Therefore, the microstructure of the samples with the lowest heat input, the highest heat input and the highest tensile strength (highest welding efficiency) was studied.

The CP-Ti base metal microstructure consists of equiaxed α particles and intergranular β phase (BCC structure). The β phase is dispersed along α phase boundaries (HCP structure). The light and dark portions represent phases of α and intergranular β, respectively, as demonstrated in Figure 4; this is consistent with what was found in some literature [22,23].

The HAZ microstructure of the A13 sample (lowest heat input) composed of acicular alpha grain gets coarser towards FZ, which was likely created by epitaxial growth during solidification, which is likely due to the increased heat input in this region compared to the base metals as shown in Figure 5. At a laser power of 0.6 kW and a welding speed of 10 mm/sec, the heat input is 24 J/mm, so the cooling rate is high, and the resulting microstructure is fine due to the lack of sufficient growth time. In addition, it has been observed that increasing the laser power to 2.5 kW and welding speed of 10 mm/s would cause an increase in the

particle size of the HAZ in the A4 specimen because of the increase in the heat input to 150 J/mm; this agrees with [24,25], as shown in Figure 6. The lack of β-α stabilisers and low cooling rate may explain why there was no martensite in the HAZ of CP-Ti; this agrees with [26].

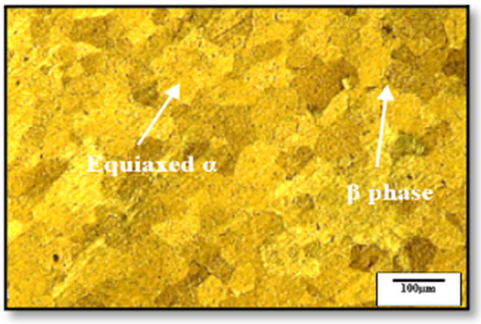

Fig. 4. CP Titanium base metal microstructure

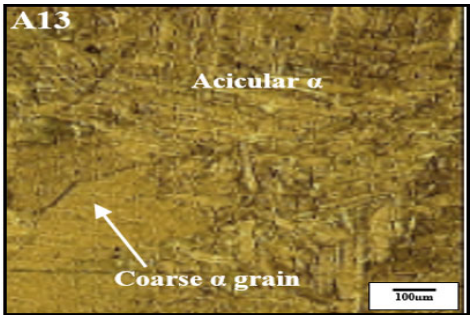

Fig. 5. Microstructure of HAZ of the A13 at the lowest heat input

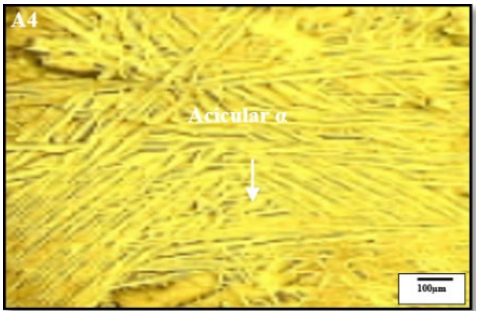

Fig. 6. Microstructure of the HAZ of the A4 at the highest heat input

Equiaxed particles were typically developed in the middle part of the FZ by growth and nucleation. In the FZ of pure metal, however, only columnar particles may develop epitaxially growth. The alloying components were thus few the growth and nucleation of equiaxed particles were not easy [23,27]. At the highest heat input, the FZ consisted mostly of a coarse acicular α due to a decrease in the cooling rate, as shown in Figure 7, while at the lowest heat input, the FZ became composed of a fine acicular α due to the increase in the cooling rate, as shown in Figure 8.

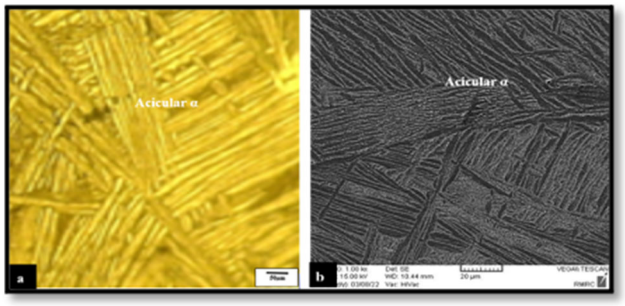

Fig. 7. The FZ microstructure of the A4 at the highest heat input by using an a) optical image, b) SEM image

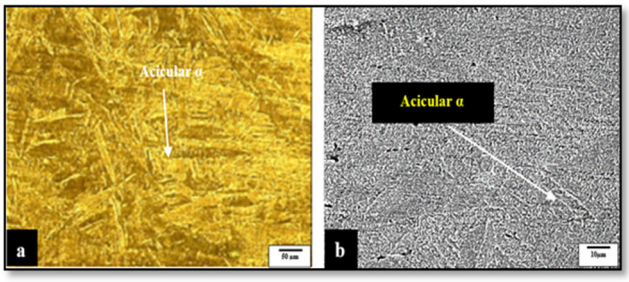

Fig. 8. The FZ microstructure of the A13 at the highest heat input using an a) optical image, b) SEM image

3.2. Influence of laser welding situations on the penetration depth of the weld and weld zone width

This test was carried out after cutting the samples into specimens with dimensions (20 * 3) mm and making moulds to easily install them in the grinding, polishing and etching processes, and then inspecting them with an electron microscope described in Chapter Three. Welding cross-sections are usually characterized by three zones (FZ, HAZ and BM) as shown in Figure 9.

Figure 10 shows the effect of changing the laser power at a low welding speed of 10mm/s on the weld penetration depth of (CP-Ti) samples welded using a fibre laser method. It shows the presence of incomplete weld penetration when the laser power is 0.6 kW as a result of insufficient heat input. The V shape formed at a low heat input of (24, 30, 36, 40, 48, 60 J/mm), while the hourglass shape formed at high heat input of (75, 80, 100, 120, 150 J/mm). When the laser

power increases, the weld penetration and weld pool width increase at a welding speed of 10 mm/s. Increasing the laser power will increase the absorption of the laser beam by the metal surface, increasing the width of the upper and lower surfaces of the FZ, which agrees with [28-31]. On the other hand, a crater was observed with all laser power values, and its depth increased with increasing laser power. The main reason is that high power or high heat input promotes evaporation and expulsion of the molten metal from the sides into the centre of the weld, which agrees with [32].

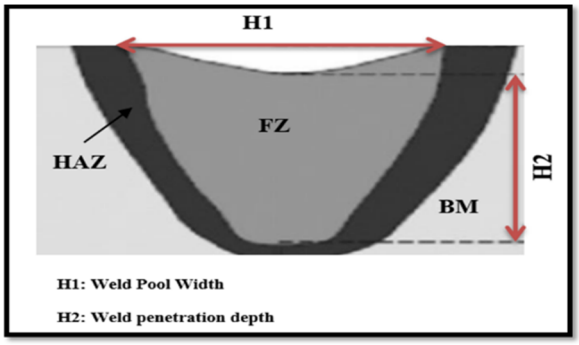

Fig. 9. Weld cross-section characterization

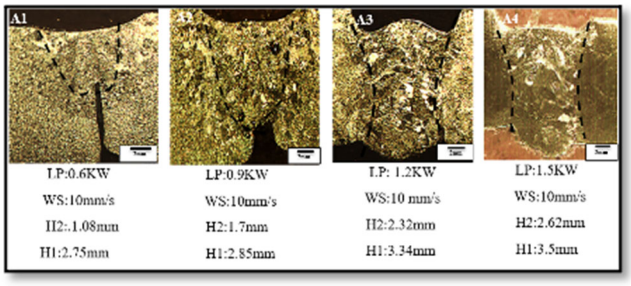

Fig. 10. the effect increases laser power on depth penetration at a welding speed of 10 mm/s of (CP-Ti) specimens

Porosity was also observed at low laser power, such as in samples of 0.6KW and 0.9KW because the heat input is low, so the shape of the weld pool is V-shaped and the cooling rate is high. As the weld metal solidifies, gas bubbles close to the surface can escape, while bubbles farther from the surface remain trapped. The porosity decreases as the laser power increase, and the weld pool turns into an hourglass shape due to the lower cooling rate. So there is time for gas bubbles to escape from the upper and lower surfaces [33].

Figures 11 and 12 show the effect of increasing welding speed on weld penetration at 1.5 kW laser power. It is observed from the figures that the depth of weld penetration decreases with the increase in the welding speed, as well as a decrease in the top and bottom weld widths. This is caused by the low heat input due to the high welding speed because there is not enough time for the laser beam to interact with the metal surface; this agrees with [29]. For FZ widths, laser power alone has proven to be more effective than welding speed. However, the HAZ was shown to be wider at lower speeds when the laser power was relatively high. In this state, the welding speed has a much greater impact on HAZ widths than laser power [33], where the weld pool turns from the shape of an hourglass to the shape of a nail head, as shown in the A12 sample. It also causes a decrease in the width of the weld pool and the HAZ [34,35], as shown in Figure 11. It was also found that crater depth decreased with increasing welding speed.

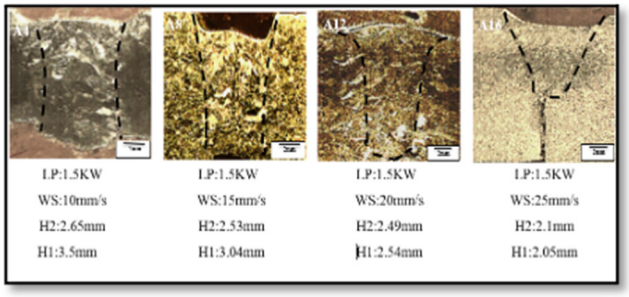

Fig. 11. The effect of increasing welding speed on depth penetration at laser power 1.5 kW

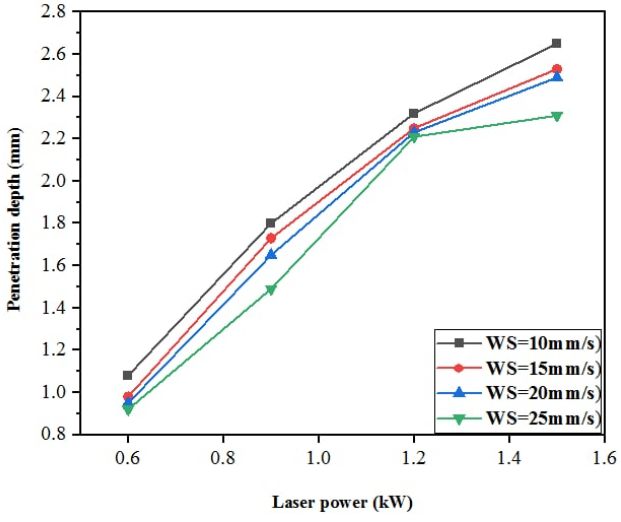

Fig. 12. Effects the laser power on weld penetration

Figure (13) shows the effect of laser power and welding speed on the width of the heat-affected zone extent from the weld centreline. It was also noted that the porosity increases

with the increase in welding speed due to the lack of time required for the gases to exit from the weld metal [23,35].

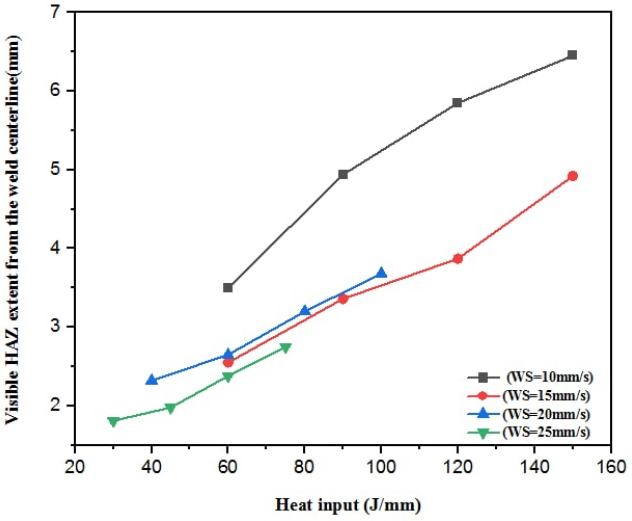

Fig. 13. Effect of the heat input on HAZ extent from the weld centreline

4. Conclusions

The weldability of Commercial production of Pure Titanium and a titanium alloy (CP-Ti) has been examined. The experiment was conducted on 0.3 cm thickness plates that were welded in a square butt welding arrangement. Utilizing a narrow fibre-laser source, the technique was carried out in continuous-wave emissions. The primary purpose of the study is on the metallurgical characterization of laser welds. It is possible to draw the next conclusions:

1. Three distinct zone has been distinguished by variations in microstructure across the welds, namely the FZ, HAZ and BM (CP-Ti).
2. B (CP-Ti) had an equiaxed microstructure in BM, but a non-uniform particle size distribution over the thickness.
3. Increasing the laser power from 0.6 kW to 1.5 kW at 10 mm/s welding speeding, the welding penetration depth increased from 1.08 mm to 2.62 mm, while increasing the welding speed significantly affected the width of the HAZ and reduced the weld penetration to 2.1 mm at 1.5 kW and 25 mm/s, due to the lack of heat input.
4. When the welding speeds increased, the HAZ and the FZ formed from a fine acicular α, which was most probably formed throughout solidification via epitaxial growth, thus the hardness increases and ductility decreases, and it is coarser at lower speeds.
5. The absence of martensite (α) phase in the weld zone was due to the lack of beta phase stabilizers.

References

[1] E. Schubert, M. Klassen, I. Zerner, C. Walz, G. Sepold, Light-Weight Structures Produced by Laser Beam Joining for Future Applications in Automobile and Aerospace Industry, Journal of Materials Processing Technology 115/1 (2001) 2-8. DOI: https://doi.org/10.1016/S0924-0136(01)00756-7

[2] R.R. Boyer, An overview on the use of titanium in the aerospace industry, Materials Science and Engineering: A 213/1-2 (1996) 103-114. DOI: https://doi.org/10.1016/0921-5093(96)10233-1

[3] C. Li, B. Li, Z. Wu, X. Qi, B. Ye, A. Wang, Stitch welding of Ti−6Al−4V titanium alloy by fiber laser, Transactions of Nonferrous Metals Society of China 27/1 (2017) 91-101. DOI: https://doi.org/10.1016/S1003-6326(17)60010-4

[4] D.S. Badkar, S.K. Pandey, G. Buvanashekaran, The Effect of Laser Beam Welding on Microstructure and Mechanical Properties of Commercially Pure Titanium, International Journal of Material Science 4/3 (2009) 299-312.

[5] M.J. Torkamany, F.M. Ghaini, E. Papan, S. Dadras, Process Optimization in Titanium Welding with Pulsed Nd:YAG Laser, Science of Advanced Materials 4/3-4 (2012) 489-496. DOI: https://doi.org/10.1166/sam.2012.1307

[6] E. Akman, A. Demir, T. Canel, T. Sinmazcelik, Laser welding of Ti6Al4V titanium alloys, Journal of Materials Processing Technology 209/8 (2009) 3705-3713. DOI: https://doi.org/10.1016/j.jmatprotec.2008.08.026

[7] BS EN 4678:2011. Aerospace series. Weldments and brazements for aerospace structures. Joints of metallic materials by laser beam welding. Quality of weldments, 2011.

[8] P. Danielson, R. Wilson, D. Alman, Microstructure of titanium welds, Advanced Material & Processes 161/2 (2003) 39-42.

[9] L. Chen, G. Shuili, J. Yang, Study on full penetration stability of light alloys sheet laser welding, Proceedings of the 37th International MATADOR Conference, Manchester, 2012, 315-318.

[10] J.D. Beguin, V. Gazagne, Y. Balcaen, J. Alexis, E. Andrieu, Laser Welding of Titanium Alloys with a Yb: YAG Disk Source, Materials Science Forum 941 (2018) 845-850. DOI: https://doi.org/10.4028/www.scientific.net/MSF.941.845

[11] M.J. Jweeg, Z.Kh. Hamdan, A.H. Majeed, K.K. Resan, M. Al-Waily, A new method for measurement the

residual stresses in friction stir welding, Archives of Materials Science and Engineering 112/2 (2021) 63-69. DOI: https://doi.org/10.5604/01.3001.0015.6285

[12] P. Omoniyi, R.A. Mahamood, N. Arthur, S. Pityana, S. Skhosane, Y. Okamoto, T. Shinonaga, M. Maina, T. Jen, E. Akinlabi, Laser Butt Welding of Thin Ti6Al4V Sheets: Effects of Welding Parameters, Journal of Composite Sciences 5/9 (2021) 246. DOI: https://doi.org/10.3390/jcs5090246

[13] Q.H. Jebur, M.J. Jweeg, M. Al-Waily, H.Y. Ahmad, K.K. Resan, Hyperelastic models for the description and simulation of rubber subjected to large tensile loading, Archives of Materials Science and Engineering 108/2 (2021) 75-85. DOI: https://doi.org/10.5604/01.3001.0015.0256

[14] E.K. Njim, S.H. Bakhy, M. Al-Waily, Analytical and numerical free vibration analysis of porous functionally graded materials (FGPMs) sandwich plate using Rayleigh-Ritz method, Archives of Materials Science and Engineering 110/1 (2021) 27-41. DOI: https://doi.org/10.5604/01.3001.0015.3593

[15] S.H. Bakhy, M. Al-Waily, M.A. Al-Shammari, Analytical and numerical investigation of the free vibration of functionally graded materials sandwich beams, Archives of Materials Science and Engineering 110/2 (2021) 72-85. DOI: https://doi.org/10.5604/01.3001.0015.4314

[16] M. Al-Waily, A.M. Jaafar, Energy balance modelling of high velocity impact effect on composite plate structures, Archives of Materials Science and Engineering 111/1 (2021) 14-33. DOI: https://doi.org/10.5604/01.3001.0015.5562

[17] E.K. Njim, S.H. Bakhy, M. Al-Waily, Free vibration analysis of imperfect functionally graded sandwich plates: analytical and experimental investigation, Archives of Materials Science and Engineering 111/2 (2021) 49-65. DOI: https://doi.org/10.5604/01.3001.0015.5805

[18] E.K. Njim, S.H. Bakhy, M. Al-Waily, Analytical and numerical flexural properties of polymeric porous functionally graded (PFGM) sandwich beams, Journal of Achievements in Materials and Manufacturing Engineering 110/1 (2022) 5-15. DOI: https://doi.org/10.5604/01.3001.0015.7026

[19] A. Abdollahi, A.S.A. Huda, S.A. Kabir, Microstructural Characterization and Mechanical Properties of Fiber Laser Welded CP-Ti and Ti-6Al-4V Similar and Dissimilar Joints, Metals 10/6 (2020) 747. DOI: https://doi.org/10.3390/met10060747

[20] X. Cao, M. Jahazi, Effect of welding speed on butt joint quality of Ti-6Al-4V alloy welded using a high-power Nd:YAG laser, Optics and Lasers in Engineering 47/11 (2009) 1231-1241. DOI: https://doi.org/10.1016/j.optlaseng.2009.05.010

[21] F. Fomin, M. Froend, V. Ventzke, P. Alvarez, S. Bauer, N. Kashaev, Metallurgical aspects of joining commercially pure titanium to Ti-6Al-4V alloy in a T-joint configuration by laser beam welding, The International Journal of Advanced Manufacturing Technology 97 (2018) 2019-2031. DOI: https://doi.org/10.1007/s00170-018-1968-z

[22] M. Junaid, N.M. Baig, M. Shamir, N.F. Khan, K. Rehman, J. Haider, A comparative study of pulsed laser and pulsed TIG welding of Ti-5Al-2.5Sn titanium alloy sheet, Journal of Materials Processing Technology 242 (2017) 24-38. DOI: https://doi.org/10.1016/j.jmatprotec.2016.11.018

[23] H. Liu, K. Nakata, J.X. Zhang, N. Yamamoto, J. Liao, Microstructural evolution of fusion zone in laser beam welds of pure titanium, Materials Characterization 65 (2012) 1-7. DOI: https://doi.org/10.1016/j.matchar.2011.12.010

[24] T.S. Auwal, S. Ramesh, F. Yusof, S.M. Manladan, A review on laser beam welding of titanium alloys, The International Journal of Advanced Manufacturing Technology 97 (2018) 1071-1098. DOI: https://doi.org/10.1007/s00170-018-2030-x

[25] X. Cao, A.S.H. Kabir, P. Wanjara, J. Gholipour, A. Birur, J. Cuddy, M. Medraj, Global and local mechanical properties of autogenously laser welded Ti-6Al-4V, Metallurgical and Materials Transactions A 45 (2014) 1258-1272. DOI: https://doi.org/10.1007/s11661-013-2106-z

[26] X. Li, J. Xie, Y. Zhou, Effects of oxygen contamination in the argon shielding gas in laser welding of commercially pure titanium thin sheet, Journal of Materials Science 40/13 (2005) 3437-3443. DOI: https://doi.org/10.1007/s10853-005-0447-8

[27] M. Cheepu, D. Venkateswarlu, P.N. Rao, S.S. Kumaran, N. Srinivasan, Effect of Process Parameters and Heat Input on Weld Bead Geometry of Laser Welded Titanium Ti-6Al-4V Alloy, Materials Science Forum 969 (2019) 613-618. DOI: https://doi.org/10.4028/www.scientific.net/MSF.969.613

[28] S. Lathabai, B.L. Jarvis, K.J. Barton, Comparison of keyhole and conventional gas tungsten arc welds in commercially pure titanium, Materials Science and Engineering: A 299/1-2 (2001) 81-93. DOI: https://doi.org/10.1016/S0921-5093(00)01408-8

[29] Y.T. Kuo, L.S. Jeng, Porosity reduction in Nd–YAG laser welding of stainless steel and Inconel alloy by

using a pulsed wave, Journal of Physics D: Applied Physics 38 (2005) 722.
DOI: https://doi.org/10.1088/0022-3727/38/5/009
[30] A. Lisiecki, Welding of titanium alloy by different types of lasers, Archives of Materials Science and Engineering 58/2 (2012) 209-218.
[31] A. Squillace, U. Prisco, S. Ciliberto, A. Astarita, Effect of welding parameters on morphology and mechanical properties of Ti–6Al–4V laser beam welded butt joints, Journal of Materials Processing Technology 212/2 (2012) 427-436.
DOI: https://doi.org/10.1016/j.jmatprotec.2011.10.005
[32] G.R. Mohammed, M. Ishak, S.N. Aqida, H.A Abdulhadi, Weld bead profile of laser welding dissimilar joints stainless steel, IOP Conference Series: Materials Science and Engineering 257 (2017) 012072. DOI: https://doi.org/10.1088/1757-899X/257/1/012072
[33] L.S. Campanelli, G. Casalino, M. Mortello, A. Angelastro, A.D. Ludovico, Microstructural characteristics and mechanical properties of Ti6Al4V alloy fiber laser welds, Procedia CIRP 33 (2015) 428-433. DOI: https://doi.org/10.1016/j.procir.2015.06.098
[34] A.S.H. Kabir, X. Cao, M. Medraj, P. Wanjara, J. Cuddy, A. Birur, Effect of Welding Speed and Defocusing Distance on the Quality of Laser Welded Ti-6Al-4V, Proceedings of the Materials Science and Technology Conference and Exhibition "MS&T 2010", Houston, Texas, 2010, 2787-2797.
[35] L.V. Murav'ev, Problems of Pore Formation in Welded Joints of Titanium Alloys, Metal Science and Heat Treatment 47/7-8 (2005) 282-288. DOI: https://doi.org/10.1007/s11041-005-0068-5